Controlling defects and secondary phases of CZTS by surfactant potassium

Yiou Zhang, Kinfai Tse, Xudong Xiao, and Junyi Zhu*
Department of Physics, The Chinese University of Hong Kong, Hong Kong SAR 999077, China
(Received 9 July 2017; published 27 September 2017)

Cu_2ZnSnS_4 (CZTS) is a promising photovoltaic absorber material with earth-abundant and nontoxic elements. However, the detrimental native defects and secondary phases of CZTS will largely reduce the energy-conversion efficiencies. To understand the origin of these problems during the growth of CZTS, we investigated the kinetic processes on CZTS $(\bar{1}\bar{1}\bar{2})$ surface, using first-principles calculations. A surface Zn atom was found to occupy the Cu site near the surface easily due to a low reaction barrier, which may lead to a high Zn_{Cu} concentration and a Zn-rich secondary phase. These *n*-type defects may create deep electron traps near the interface and become detrimental to device performance. To reduce the population of Zn_{Cu} and the Zn-rich secondary phase, we propose to use K as a surfactant to alter surface kinetic processes. Improvements on crystal quality and device performance based on this surfactant are consistent with early experimental observations.

DOI: 10.1103/PhysRevMaterials.1.045403

I. INTRODUCTION

Cu_2ZnSnS_4 (CZTS), as a promising thin-film solar-cell material, has drawn great attention in the past few years [1–9]. With a zinc-blende-derived kesterite structure, CZTS has a high absorption coefficient and a direct band gap of 1.5 eV, close to the optimal value for single-junction solar-cell materials [10]. Moreover, all the elements in CZTS are nontoxic and earth-abundant [11–14], and the efficiency of a solar cell based on an alloy of CZTS and $Cu_2ZnSnSe_4$ has reached 12.6% [15]. However, the narrow stable chemical-potential range of CZTS [12,13,16] leads to detrimental defects and phase inhomogeneity, which have been observed experimentally [3,10,17–19]. Also, the presence of detrimental defects in CZTS may form recombination centers that limit the energy-conversion efficiency.

For thin-film solar-cell materials, modifications of surface properties are important for both material growth and photovoltaic performance [3,8,17,20–22]. However, the surface properties of CZTS are difficult to study due to the polycrystalline nature of this thin film. X-ray diffraction patterns indicate that the most favorable orientation of CZTS growth is $(112)/(\bar{1}\bar{1}\bar{2})$ for both sputtering [23,24] and coevaporation [17], and that the S-terminated $(\bar{1}\bar{1}\bar{2})$ surface has the lowest surface energy [14]. The most stable surface reconstruction under Cu-poor and Zn-rich condition is a $(1 \times 1)\,2Zn_{Cu}$ reconstructed surface, where all the Cu sites in the first cation layer of CZTS are occupied by Zn atoms [14], resulting in the Cu-depleted region near surfaces, as observed in experiments [25]. As $(\bar{1}\bar{1}\bar{2})$ surface is the most abundant surface in CZTS thin films from both experimental and theoretical studies, we will focus on $(\bar{1}\bar{1}\bar{2})$ surface in this paper. Other surface orientations could also exist, yet investigation of them is out of the scope of this paper.

Besides these thermodynamic properties, surface kinetics may play an important role in CZTS growth due to the low growth temperature [8,15,17], but the kinetic process that leads to the reconstruction during crystal growth remains unknown. Moreover, the effects of surface kinetic processes on defects and secondary phase formation are not studied. To propose effective surface growth techniques, it is essential to first understand the formation kinetics of the native defects and secondary phase near the surface. As direct observation of surface processes is hard in experiments, if not impossible, first-principles calculations become attractive. Moreover, since first-principles calculations show good consistency with experimentally observed surface properties of CZTS [14,17,23–25], they are also expected to capture the critical processes on the CZTS surface.

According to our surface kinetic analysis, Zn-rich secondary phases are of special importance because they are likely to form near the CZTS $(\bar{1}\bar{1}\bar{2})$ surface kinetically, and Zn_{Cu} may accumulate near the interface. To suppress the detrimental phases of Cu_2S, CuS, and Cu_xSnS_y [26,27], the growth is usually under Cu-poor and Zn-rich conditions [2,11,15]. Such growth conditions also provide a thermodynamic driving force to form ZnS or other Zn-rich secondary phases. Due to the similar crystal structures and lattice constants between ZnS and CZTS, it is difficult to characterize ZnS phase in CZTS as the two x-ray diffraction patterns overlap [27]. Although a coherent interface between CZTS and ZnS may exist, and a type-I band offset between CZTS and ZnS is believed to be electronically benign [28], electronic properties of Zn_{Cu} defects near the interface were not well studied and may have detrimental effects, as our further analysis shows.

To reduce the secondary phases and detrimental defects, surface modifications are appealing in the growth of semiconductors [8,14,17]. Based on understandings of surface thermodynamics and kinetics, surface growth techniques, such as surfactants, can be used to modify the surface morphology and change the surface electronic structures [23,25,26,29–31]. Surfactant elements are elements that always flow on top of the growing front [29–33]. Although surfactants are used in group III–V semiconductors [29–32,34], surfactant effect on CZTS has not been thoroughly studied. Recently it was proven experimentally that surfactant effect of Na in coevaporation growth of CZTS can enlarge the grain size and suppress formation of ZnS secondary phase near the surface [35]. This shows that surfactant effect may also play an important role in CZTS growth. Also, it was found in experiments that a

*jyzhu@phy.cuhk.edu.hk

small amount of K incorporation in CZTS can enhance the formation of (112) surfaces, increase the grain size, reduce ZnS secondary phase, and increase the short-circuit current [36]. Nevertheless, the physical origin remains unknown. Since it is very difficult to directly observe the surface kinetic process during the growth, first-principles calculations are attractive tools to study this problem.

In this paper, to answer all the questions raised above, we studied (1) the diffusion kinetic processes of Zn, Cu near the CZTS $(\bar{1}\bar{1}\bar{2})$ surface; (2) the electronic properties of Zn_{Cu} at the interface between CZTS and ZnS; and (3) the surfactant effect of K on CZTS, using first-principles approaches. First, we showed that an intrinsic surface kinetic process will lead to the formation of undesirable Zn_{Cu} defect and Zn-rich secondary phases. Our calculations showed that there is only a small energy barrier to form the $(1 \times 1)\,2Zn_{Cu}$ reconstructed surface, whereas the recovery to stoichiometric surfaces is more difficult. These results indicate that a large number of n-type Zn_{Cu} may be buried into the bulk from the surface, and Zn-rich secondary phases may be formed. Additionally, our calculations showed that despite the shallow nature of the Zn_{Cu} antisite defect in bulk CZTS, such antisite defect may create deep electron traps on the interface between CZTS and ZnS. These active electron traps will greatly limit the efficiency of CZTS. Further, we showed that K can alter such intrinsic surface processes and improve the crystal quality. By changing surface electronic environment and kinetic processes, K adatoms can largely suppress the formation of Zn_{Cu} near the surface and increase the diffusion length of Zn adatoms. Therefore, the population of undesirable Zn_{Cu} defects will be reduced and the Zn-rich secondary phases will be suppressed, consistent with experiment results [36]. Moreover, K atoms in bulk CZTS will most likely take Zn sites instead of commonly believed Cu sites [36], creating a shallow acceptor level and thus being electronically benign. Therefore, a small amount of K incorporation is in fact beneficial for the device performance of CZTS.

II. CALCULATION DETAILS

The total energy calculations of bulks and slabs were based on density-functional theory [37,38] as implemented in VASP code [39,40], with a plane-wave basis set [41,42]. The energy cutoff of the plane wave was set at 400 eV and Perdew-Burke-Ernzerhof generalized gradient approximation (GGA) functional [43] was used. For surface calculations, (2×1) unit cell slabs containing six bilayers of CZTS and at least 15 Å vacuum are used. A $(3 \times 3 \times 1)$ Monkhorst-Pack [44] k-point mesh was used for integration over the Brillouin zone. Convergence tests with respect to energy cutoff of plane wave, k-point sampling, slab, and vacuum thickness have been explicitly performed. These tests show that the total energies of the slab structures have converged to approximately 0.1 eV, and relative energies between different slab structures have converged to approximately 0.01 eV due to further error cancellations among these structures. Pseudohydrogen atoms with charge $q = 1.75e$,$q = 1.5e$, and $q = e$ were added on the bottom surface to passivate dangling bonds of Cu, Zn, and Sn atoms. Atoms were relaxed until force converged to less than 0.01 eV/Å. Transition-state energy was determined by the climbing-image nudged elastic band method [45]. The number of images along the diffusion path is chosen to satisfy the criterion that the distances between neighboring images are approximately 0.5 Å to further reduce the systematic error. Bulk defect properties were obtained using a supercell approach, where single defect was introduced in a 512-atom cell with Γ-point-only k-point sampling. Single-electron energy levels of different defects and charge states were aligned using energy levels of core electrons far away from the defect. The use of large supercell allows accurate determination of both relaxation energy and defect level [46,47], matching experimental defect concentration.

III. RESULTS AND DISCUSSION

A. Surface kinetics of Zn and Cu

We first demonstrated the kinetic process of the invasion of Cu sites in the first cation layer of the unreconstructed $(\bar{1}\bar{1}\bar{2})$ surface by adatom Zn. Due to low symmetry of CZTS, there are four inequivalent $H3$ sites and four inequivalent $T4$ sites, and absorption of Zn adatom on these sites shows different behaviors. Exhaustive testing on $H3$ and $T4$ sites shows that Zn adatom is stable except for the $T4$ site above Sn atom, which will spontaneously relax toward a neighboring $H3$ site due to the size effect of Sn atoms. Remarkably, significant distortion on Cu atom, as shown in Fig. 1(b), is observed when Zn adatom is on the $T4$ site above Cu atoms. At energy minimum, Zn adatom is nearly coplanar with S atoms, while the Cu atom below is bonded to only three S atoms. Stability of such structure is due to the larger atomic size of Zn and Zn-S bonding being stronger than Cu-S bonding. Energy is gained during the stabilization of the Zn adatoms and the destabilization of the Cu atoms below. Comparatively, Zn adatoms on $H3$ sites, lacking such kind of energy-gain mechanism, are less stable by at least 0.4 eV. As a result, the adsorption of Zn adatom at $T4$ site above a Cu atom is the most stable configuration.

Since the Cu atoms below Zn adatoms become loosely bonded, they are more likely to diffuse away, and the Zn adatoms will occupy the Cu sites and form Zn_{Cu}. Such diffusion will result in an exchange between the Zn adatoms and the Cu atoms below the Zn adatoms, as shown in Fig. 1(a). As can be seen from the figure, the energy barrier of the exchange process is only 0.25 eV, comparable to the diffusion barrier of Zn adatoms on the surface. Moreover, there will be a significant energy gain when a Zn adatom occupies the Cu site (0.7 eV compared with a Zn adatom on an $H3$ site). Therefore, Cu atoms in the first cation layer act as traps of Zn adatoms on the surface, and it is likely that a high population of Zn_{Cu} may accumulate near the surface. Moreover, as the diffusion length of Zn adatoms is significantly limited by these Cu atoms, the distribution of Zn on the surface might become highly inhomogeneous. As a consequence, Zn-rich secondary phases instead of normal CZTS would be formed in the Zn-rich region, while CZTS may only be formed in some Zn-poor region. Our calculation indicates that at the very early stage of the growth, in addition to the thermodynamic driving force, there exists a

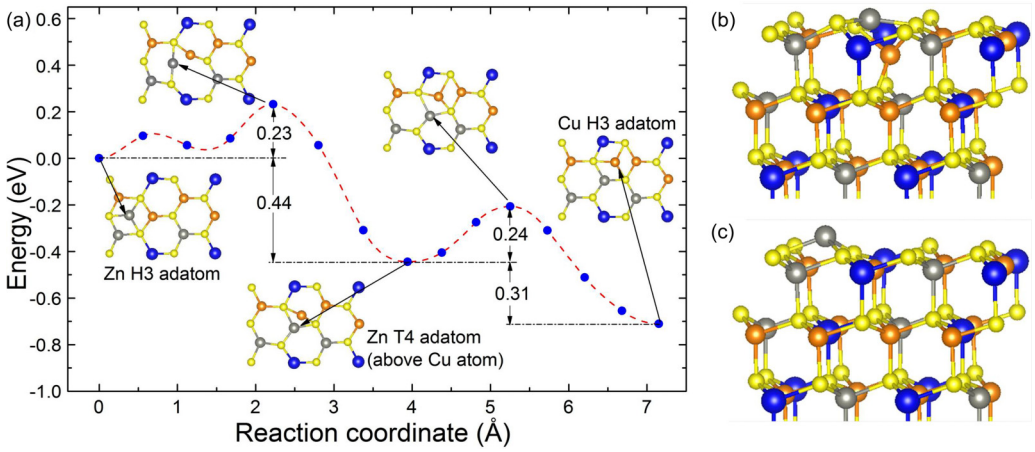

FIG. 1. (a) Reaction barriers for a Zn adatom on $H3$ site diffusing to $T4$ site and then replacing the Cu atom below. The orange, white, blue, and yellow balls show Cu, Zn, Sn, and S in order. Potential energy profile is displayed by the red curve, and arrows point toward the adatom on top of the surface for the specified configurations (blue dots). Energy differences between local minimums and saddle points are labeled in the figure. Side views of Zn adatom on $T4$ and $H3$ sites are shown in (b) and (c).

kinetic driving force to form Zn_{Cu} near the surface, which may lead to formation of Zn-rich secondary phases.

Further, we studied the kinetics of Cu adatoms on the $(1 \times 1)\,2Zn_{Cu}$ reconstructed surface. The most stable adsorption site for a Cu adatom is one of the $H3$ sites, which has the largest distance away from the Sn atoms in the cation layer. When Cu adatoms occupy the Cu sites, the replaced Zn atoms still favor $T4$ sites above the Cu atoms. As shown in Fig. 2, such a replacement is unfavorable both kinetically and thermodynamically, as the reaction barrier is more than 0.5 eV and the energy of the final stage is nearly 0.3 eV higher than that of the initial stage. Although the kinetic barrier may not be high under growth temperature of CZTS, the replacement is still hindered by the energy difference between the initial and final configurations. This result indicates that the $(1 \times 1)\,2Zn_{Cu}$ reconstructed surface remains stable during further growth,

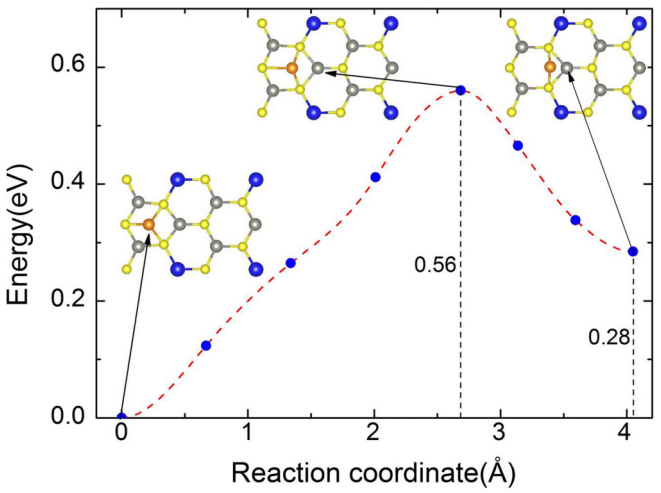

FIG. 2. Reaction barrier for Cu adatom replacing one Zn_{Cu} in the cation layer. Arrows point toward adatom on top of the surface for specified configuration (blue dots). Energies of the saddle point and the final configuration relative to the initial configuration are labeled in the figure.

and it is hard to remove the Zn_{Cu} near the surface from both thermodynamic and kinetic aspects. Since the diffusion barrier of Zn_{Cu} is approximately 2 eV in bulk CZTS according to our unpublished results, it is even harder to remove such antisites when they are buried in bulk. Therefore, there might be a high population of Zn_{Cu} in bulk CZTS due to surface kinetic processes.

B. Electronic properties of Zn_{Cu} at the interface between ZnS and CZTS

Due to the limited diffusion length of Zn adatom on CZTS surface and the Zn-rich condition during the growth, Zn-rich secondary phases are likely to form. Although the exact structures and composition of these secondary phases could be complex, these secondary phases can be approximately treated as doped ZnS. The ZnS secondary phase was believed to be electronically benign due to its lattice-matched structure and type-I band alignment [26]. However, such kind of benign properties exist only when the interface between CZTS and ZnS is defect-free. If this doped ZnS is formed on top of the $(1 \times 1)\,2Zn_{Cu}$ reconstructed CZTS surface (which is likely during the CZTS growth), one layer of ordered defects may be formed on the interface. Such defects will be almost frozen on the interface due to the high kinetic barrier of Zn_{Cu} in bulk CZTS, resulting in high defect concentrations near the interface.

To understand the electronic properties of the defects on the interface, we constructed a (1×1) unit cell along the [112] direction of CZTS, containing nine bilayers of CZTS and nine bilayers of ZnS, to simulate this interfaces between CZTS and Zn-rich secondary phases. Although there are two inequivalent interfaces in the supercell, they are charge-neutral and can be regarded as fully separated. The average interface energy is only 1.5 meV/Å^2, suggesting that the interface is almost stress-free without any charge transfer. Then Zn_{Cu} on one interface was simulated, and the obtained electronic structure is shown in Fig. 3(a). As can be seen from the density-of-states plot, a deep gap state exists when one layer of defects is created on

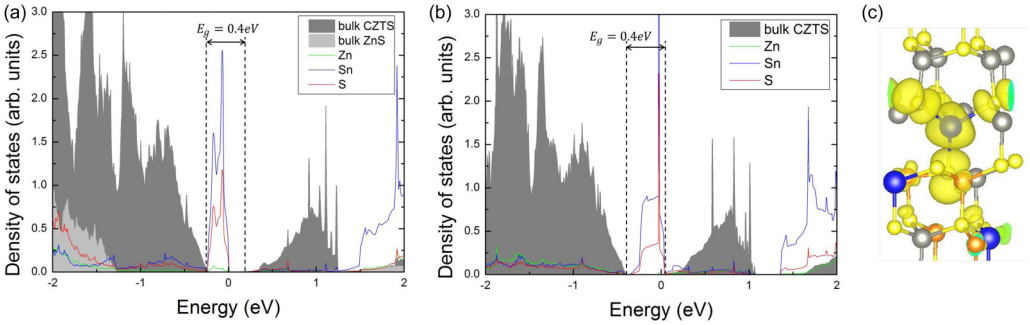

FIG. 3. Partial density of states for one layer of Zn_{Cu} antisite defects (a) on the interface between CZTS and ZnS and (b) inside CZTS. Fermi energy is set as zero. Shaded areas with dark and light gray color represent the density of states of bulk CZTS and ZnS, respectively, determined from atoms far away from the interface. Green, blue, and red lines indicate partial density of states projected around Zn, Sn, and S atoms on the defect layer. The band gap of the bulk CZTS is indicated in (a) and (b). (c) shows the partial charge density of the gap state in (a).

the interface. Although the defects are *n* type in nature, the gap state is actually close to the valence-band maximum (VBM) of CZTS, partly due to an underestimation of band gap by GGA functional (the band gap of CZTS is around 0.4 eV from our calculations, much smaller than the band gap of 1.5 eV from experiments). Interestingly, Zn atoms have little contribution to the gap state, and the partial charge density shown in Fig. 3(c) indicates that the gap state is an antibonding state between Sn *s* orbital and S *p* orbital. These findings suggest that the defect layer can be regarded as a ZnS layer with ordered Sn_{Zn} defect.

We also studied the defect layer formed inside CZTS, as CZTS may also grow on the reconstructed surface. The calculation was done using a similar supercell with all ZnS bilayers replaced by CZTS bilayers, and the electronic structure is shown in Fig. 3(b). Similar to that on the CZTS-ZnS interface, the defect layer inside CZTS also creates a gap state originating from Sn and S atoms on the defect layer. Again, the defect layer can be regarded as one layer of Sn-doped ZnS inside CZTS. Combining the calculations of Zn_{Cu} defect layer on CZTS-ZnS interface and in bulk CZTS, we may conclude that under high concentration of Zn_{Cu} defects, the donor electrons would transfer to a neighboring Sn atom, and local structure tends to transform into Sn-doped ZnS. Effectively, some Sn_{Zn} defects would be created, and the donor level becomes much deeper. Although Zn_{Cu} has a relatively high defect-formation energy and only creates shallow donor level in bulk CZTS [13,16], local concentration of Zn_{Cu} could be high due to the surface kinetic process. As a consequence, some deep-level defects might be formed, particularly near the interface between CZTS and Zn-rich secondary phases. Eventually, they change the benign interface into a detrimental one. Although the concentration of Zn_{Cu} defects may not reach such a high level, we believe that the deep nature of such defects near the interface is still qualitatively correct.

From the above calculations, we found that the charge-compensating effects can significantly lower the formation energy of the *n*-type Zn_{Cu} on the electron-poor S-terminated surface, while it is about 2 eV [11–13] in the bulk. Moreover, the difference in the bond strength and atomic size between Cu and Zn results in a low reaction barrier for the formation of Zn_{Cu}, but a much higher barrier for the removal of such defects. This intrinsic surface process would lead to the accumulation of Zn_{Cu} near the surface, and some of them may eventually be buried into the bulk. High concentrations of such defects near interfaces with Zn-rich secondary phases or grain boundaries could create deep electron traps, significantly lowering the device performance. To suppress the formation of these undesirable defects, it is important to alter both the electronic environment and the kinetic process on CZTS surfaces.

C. Potassium as a surfactant to reduce Zn_{Cu} and ZnS

One of the effective approaches to modify the electronic environment and the kinetic process near surfaces is to incorporate surfactants. The surfactant elements are often large atoms that are difficult to diffuse into the bulk. At the same time, surfactants should help satisfy the electron-counting rule (ECR) [48–50] to lower the total energy. K atoms may serve ideally for these two purposes.

First, we calculated the formation energy of K-related defects in bulk. To understand the defect properties of K substitutional and interstitial defects, we surveyed the formation-energy and transition-energy level of defects at all inequivalent configurations, with chemical-potential range shown in Fig. 4. Our computed stable chemical-potential range and properties for selected intrinsic defects show qualitative agreement with previous work [13]. Various phases from K_2S to K_2S_6 have been considered to determine the rich limit of K

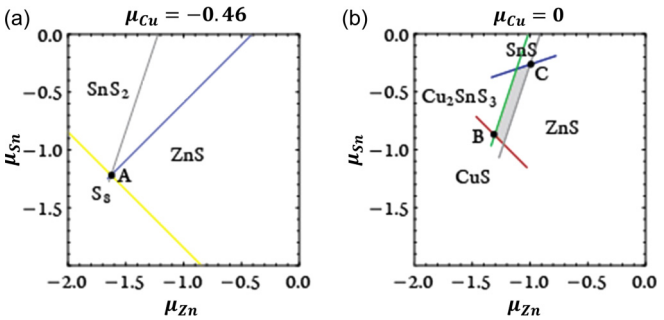

FIG. 4. Stable chemical potential range of Cu_2ZnSnS_4 at (a) Cu-poor and (b) Cu-rich limit. The bounding secondary phases are indicated in the figure. Point A indicates Cu-poor limit, whereas points B and C represent, respectively, Zn-poor and Zn-rich limit under Cu-rich condition.

TABLE I. Formation energies (in units of eV) of K-related defects. Chemical potentials of Cu, Zn, Sn, and S are chosen from the representative points of stable chemical potential range, labeled in Fig. 4. The corresponding chemical potential ($\mu_{Cu}/\mu_{Zn}/\mu_{Sn}/\mu_K$) are listed in parentheses in units of eV.

Chemical potential condition	K_{Cu}	K_{Zn}	K_{Sn}	K_i
A(−0.46/−1.63/−1.22/−2.16)	1.57	1.35	2.42	–
B(0.00/−1.31/−0.88/−1.47)	1.37	1.08	2.09	–
C(0.00/−1.00/−0.27/−1.27)	1.17	1.19	2.51	–

under different chemical-potential conditions of CZTS. Table I lists the formation energy at a selected point in the stable chemical-potential range, and the chemical potential of K is taken at the rich limit. Even under such K-rich condition, high formation energies for all K-related defects have been observed, particularly under the Cu-poor condition. Contrary to Na-doped $Cu_2InGaSe_4$, where Na_{Cu} is thermodynamically favored [51], we found that K_{Zn} substitutional defect is at least as stable on the Zn-richest limit, and generally more stable over the whole chemical-potential range. It is also worth noting that K_i will relax simultaneously into K_{Cu} and Cu_i, which may significantly reduce local stress; thus such configuration is unstable. The K_{Zn} defect has a $(-1/0)$ transition level of 0.045 eV, possibly providing p-type carrier at room temperature. It can therefore be concluded that a high concentration of K defect in bulk CZTS is unlikely, and that the trace amount of K inevitably incorporated is driven thermodynamically and kinetically into benign K_{Zn} substitutional defects.

Then we studied the surfactant effects of K on surfaces. Since K atoms will donate electrons to the electron-poor surface, the formation of Zn_{Cu} may be suppressed thermodynamically. To verify this assumption, we studied the effects of K surfactant on the $(\bar{1}\bar{1}\bar{2})$ surface of CZTS. The two K adatoms were put on each (1×1) unit cell to satisfy ECR [48–50]. All possible configurations for K adatoms were searched, and the most stable configuration is shown in Fig. 5(a). The energy costs for exchanging K adatoms with Cu, Zn, and Sn atoms are 0.80, 0.36, and 1.26 eV, respectively, suggesting that K tends to segregate on the surface rather than incorporating into bulk. The relatively small exchange energy of K and Zn is consistent with our bulk calculations.

Since the distance between the nearest K atoms is 4.58 Å, the same as that in bulk K, a metallic bond may form along the one-dimensional (1D) chain, as confirmed by the electronic structure calculation shown in Figs. 5(b) and 5(c). Electrons in this metallic surface state are transferred to dangling bonds of S atoms, leaving an empty state above the VBM. Since all dangling bonds of S atoms are fully occupied, cation adsorption on the surface is much weaker. The adsorption energy of a Zn adatom is 1.55 eV higher than that on an unreconstructed surface, and the Zn adatom is only bonded to one S atom. Also, the formation energy of Zn_{Cu} is increased by 0.79 eV, as the surface is no longer electron-poor. Similarly, formation energy of Sn_{Zn} antisite, which is a detrimental n-type defect, is increased by 1.61 eV. Formation energies of other n-type defects are also expected to be higher on the K-capped surface. Moreover, there are no noticeable relaxations for cation atoms when a Zn adatom is adsorbed, indicating that all atoms in the CZTS bilayer remain tightly bonded. Indeed, our surface kinetics calculations, as shown in Fig. 6, revealed that diffusion barriers of a Zn adatom on the K-capped surface are less than 0.35 eV, while the reaction barrier of a Zn adatom incorporating into the Cu site in the cation layer is 1.31 eV, much higher than that on bare surface. Moreover, such incorporation process is thermodynamically less favorable, as the final configuration (Cu adatom) is 0.15 eV higher than the initial one (Zn adatom).

As the formation of Zn_{Cu} near the surface is suppressed both thermodynamically and kinetically, fewer electron traps will be formed inside CZTS and on the grain boundary, which might be the reason behind the enhancement of short-circuit current by K doping [36]. Also, the mean diffusion length for a Zn adatom is expected to be much longer on K-capped surfaces than that on bare surfaces. As a consequence, Zn-rich secondary phases are unlikely to form, and the grain size of CZTS could become larger, as observed in experiments [36].

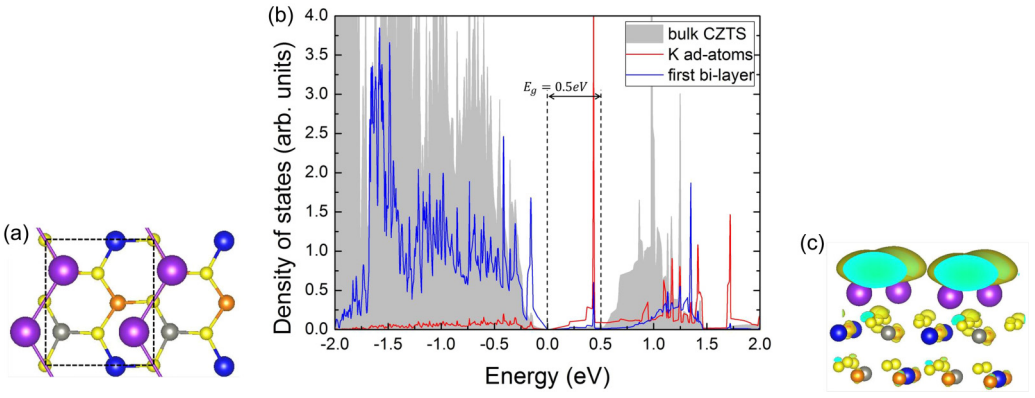

FIG. 5. (a) Top view of the most stable configuration for two K adatoms per (1×1) cell. Purple balls represent K and dashed line indicates (1×1) cell. (b) Partial density of states for K-capped CZTS surface. Shaded area represents density of states of bulk CZTS, determined from atoms far away from surface. Red (blue) lines represent partial density of states projected around K adatoms (atoms in first bilayer on the surface). (c) Partial charge density of the surface state in the band gap of bulk CZTS, as indicated in (b).

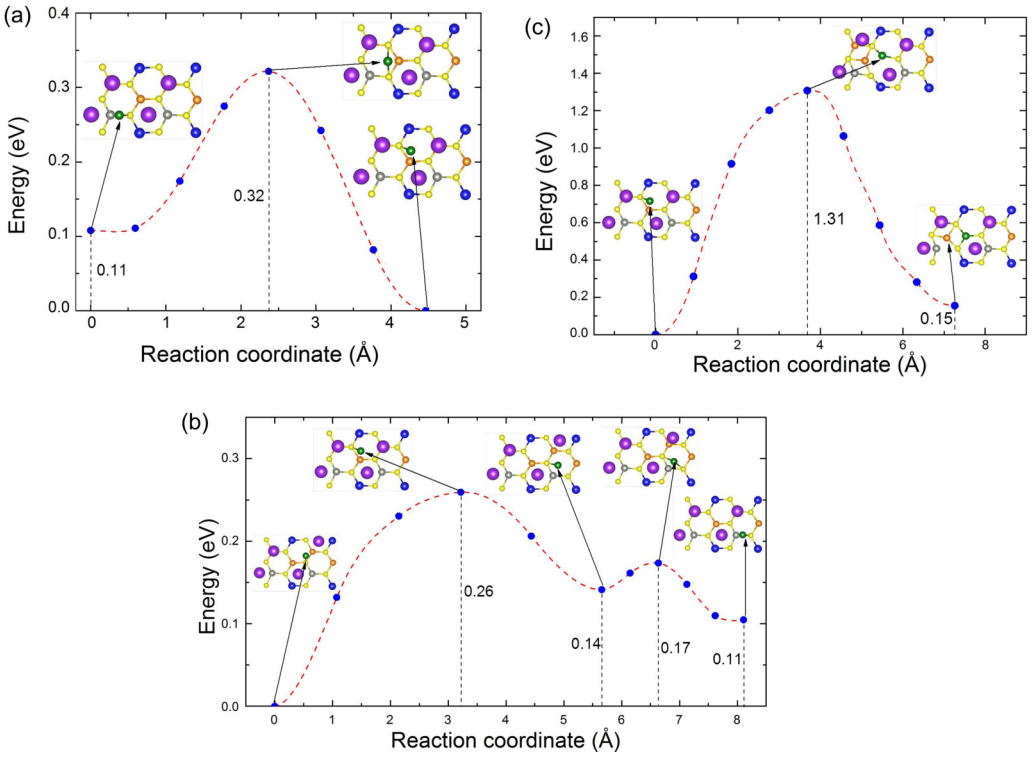

FIG. 6. Reaction path of Zn adatom on K-capped CZTS surface at different locations (blue dots). Surface diffusion paths of Zn adatom along and across the 1D chain of K adatoms are shown in (a) and (b), respectively, and incorporation of Zn adatom into Cu site in the cation layer is shown in (c). Zn adatom is represented by green balls for clarity. Energy of Zn adatom at the most stable adsorption site is set as zero, and relative energies of other saddle-point- and end-point configurations are labeled in the figure.

IV. SUMMARY

In summary, we have studied the intrinsic surface kinetic processes on S-terminated $(\bar{1}\bar{1}\bar{2})$ surface of CZTS, and investigated the surfactant effect of K on this surface. The low reaction barrier of Zn_{Cu} formation on CZTS surface may result in high concentration of such defects in the bulk and the formation of Zn-rich secondary phases. These defects may create deep electron traps inside CZTS and on the interface between CZTS and ZnS, largely reducing the efficiency of CZTS solar cell. The K atoms on CZTS surface can act as a surfactant to greatly reduce the formation of the Zn_{Cu}, and alter the intrinsic surface kinetic processes. As a result, the formation of Zn_{Cu} and Zn-rich secondary phases can be largely suppressed, consistent with experimental results. It should be noted that the polycrystalline nature and low symmetry of CZTS makes it difficult, if not impossible, to include all possible processes into consideration. Some important processes might be missed in our studies. Nevertheless, the surface processes we have found are likely to be critical for the quality of CZTS thin film, and the surfactant effect of K is worth further investigation. Our findings also suggest that large metallic group I elements may act as ideal surfactants on electron-poor surfaces to reduce the formation of detrimental native defects and secondary phases, and greatly enhance the performance of quaternary compound photovoltaic devices.

ACKNOWLEDGMENTS

We would like to thank Bei Deng and Michael Scarpulla for helpful discussions. Computing resources were provided by the High Performance Cluster Computing Centre, Hong Kong Baptist University. This work was supported by the start-up funding at CUHK. Financial support of General Research Fund (Grant No. 2130490) and Research Incentive Scheme (Grant No. 4441641) from the Research Grants Council in Hong Kong is gratefully acknowledged.

[1] T. K. Todorov, J. Tang, S. Bag, O. Gunawan, T. Gokmen, Y. Zhu, and D. B. Mitzi, Adv. Energy Mater. **3**, 34 (2013).
[2] D. B. Mitzi, O. Gunawan, T. K. Todorov, K. Wang, and S. Guha, Sol. Energy Mater. Sol. Cells **95**, 1421 (2011).
[3] S. Siebentritt, N. Papathanasiou, J. Albert, and M. C. Lux-Steiner, Appl. Phys. Lett. **88**, 151919 (2006).
[4] A. Walsh, S. Chen, S. Wei, and X. Gong, Adv. Energy Mater. **2**, 400 (2012).
[5] H. Wang, Int. J. Photoenergy **2011**, 801292 (2011).
[6] A. Weber, S. Schmidt, D. Abou-Ras, P. Schubert-Bischoff, I. Denks, R. Mainz, and H. Schock, Appl. Phys. Lett. **95**, 041904 (2009).
[7] C. Steinhagen, M. G. Panthani, V. Akhavan, B. Goodfellow, B. Koo, and B. A. Korgel, J. Am. Chem. Soc. **131**, 12554 (2009).
[8] A. Redinger and S. Siebentritt, Appl. Phys. Lett. **97**, 092111 (2010).

[9] J. Zhu, F. Liu, and M. A. Scarpulla, APL Mater. **2**, 012110 (2014).
[10] D. Park, D. Nam, S. Jung, S. An, J. Gwak, K. Yoon, J. H. Yun, and H. Cheong, Thin Solid Films **519**, 7386 (2011).
[11] S. Chen, A. Walsh, X. Gong, and S. Wei, Adv. Mater. **25**, 1522 (2013).
[12] S. Chen, X. Gong, A. Walsh, and S. Wei, Appl. Phys. Lett. **96**, 021902 (2010).
[13] S. Chen, J. H. Yang, X. G. Gong, A. Walsh, and S. H. Wei, Phys. Rev. B **81**, 245204 (2010).
[14] P. Xu, S. Chen, B. Huang, H. J. Xiang, X. G. Gong, and S. H. Wei, Phys. Rev. B **88**, 045427 (2013).
[15] W. Wang, M. T. Winkler, O. Gunawan, T. Gokmen, T. K. Todorov, Y. Zhu, and D. B. Mitzi, Adv. Energy Mater. **4**, 1301465 (2014).
[16] D. Han, Y. Y. Sun, J. Bang, Y. Y. Zhang, H. B. Sun, X. B. Li, and S. B. Zhang, Phys. Rev. B **87**, 155206 (2013).
[17] T. Tanaka, D. Kawasaki, M. Nishio, Q. Guo, and H. Ogawa, Phys. Status Solidi C **3**, 2844 (2006).
[18] K. Wang, B. Shin, K. B. Reuter, T. Todorov, D. B. Mitzi, and S. Guha, Appl. Phys. Lett. **98**, 051912 (2011).
[19] X. Fontané, L. Calvo-Barrio, V. Izquierdo-Roca, E. Saucedo, A. Pérez-Rodriguez, J. Morante, D. Berg, P. Dale, and S. Siebentritt, Appl. Phys. Lett. **98**, 181905 (2011).
[20] A. Hofmann and C. Pettenkofer, Surf. Sci. **606**, 1180 (2012).
[21] J. E. Jaffe and A. Zunger, Phys. Rev. B **64**, 241304 (2001).
[22] S. B. Zhang and S. H. Wei, Phys. Rev. B **65**, 081402 (2002).
[23] P. Fernandes, P. Salomé, and A. Da Cunha, Thin Solid Films **517**, 2519 (2009).
[24] P. Fernandes, P. Salomé, and A. Da Cunha, Semicond. Sci. Technol. **24**, 105013 (2009).
[25] M. Bär, B. Schubert, B. Marsen, S. Krause, S. Pookpanratana, T. Unold, L. Weinhardt, C. Heske, and H. Schock, Appl. Phys. Lett. **99**, 112103 (2011).
[26] B. G. Mendis, M. C. Goodman, J. D. Major, A. A. Taylor, K. Durose, and D. P. Halliday, J. Appl. Phys. **112**, 124508 (2012).
[27] C. Platzer-Björkman, J. Scragg, H. Flammersberger, T. Kubart, and M. Edoff, Sol. Energy Mater. Sol. Cells **98**, 110 (2012).
[28] A. Nagoya, R. Asahi, and G. Kresse, J. Phys.: Condens. Matter **23**, 404203 (2011).
[29] J. Zhu and S. Wei, Front. Mater. Sci. **5**, 335 (2011).
[30] J. Zhu, G. Stringfellow, and F. Liu, in APS Meeting Abstracts, 2009, p. 21012.
[31] J. Y. Zhu, F. Liu, and G. B. Stringfellow, Phys. Rev. Lett. **101**, 196103 (2008).
[32] J. Zhu, F. Liu, and G. Stringfellow, J. Cryst. Growth **312**, 174 (2010).
[33] M. Copel, M. C. Reuter, E. Kaxiras, and R. M. Tromp, Phys. Rev. Lett. **63**, 632 (1989).
[34] C. Fetzer, R. Lee, J. Shurtleff, G. Stringfellow, S. Lee, and T. Seong, Appl. Phys. Lett. **76**, 1440 (2000).
[35] T. Gershon, B. Shin, N. Bojarczuk, M. Hopstaken, D. B. Mitzi, and S. Guha, Adv. Energy Mater. **5**, 1400849 (2015).
[36] Z. Tong, C. Yan, Z. Su, F. Zeng, J. Yang, Y. Li, L. Jiang, Y. Lai, and F. Liu, Appl. Phys. Lett. **105**, 223903 (2014).
[37] P. Hohenberg and W. Kohn, Phys. Rev. **136**, B864 (1964).
[38] W. Kohn and L. J. Sham, Phys. Rev. **140**, A1133 (1965).
[39] G. Kresse and J. Hafner, Phys. Rev. B **49**, 14251 (1994).
[40] G. Kresse and J. Furthmüller, Comput. Mater. Sci. **6**, 15 (1996).
[41] P. E. Blöchl, Phys. Rev. B **50**, 17953 (1994).
[42] G. Kresse and D. Joubert, Phys. Rev. B **59**, 1758 (1999).
[43] J. P. Perdew, K. Burke, and M. Ernzerhof, Phys. Rev. Lett. **77**, 3865 (1996).
[44] H. J. Monkhorst and J. D. Pack, Phys. Rev. B **13**, 5188 (1976).
[45] G. Henkelman, B. P. Uberuaga, and H. Jónsson, J. Chem. Phys. **113**, 9901 (2000).
[46] S. Wei, Comput. Mater. Sci. **30**, 337 (2004).
[47] G. Makov, R. Shah, and M. C. Payne, Phys. Rev. B **53**, 15513 (1996).
[48] M. D. Pashley, Phys. Rev. B **40**, 10481 (1989).
[49] D. Chadi, J. Vac. Sci. Technol. A **5**, 834 (1987).
[50] W. A. Harrison, J. Vac. Sci. Technol. **16**, 1492 (1979).
[51] S. Wei, S. Zhang, and A. Zunger, J. Appl. Phys. **85**, 7214 (1999).